Cytosolic NADPH Homeostasis in Glucose-starved Procyclic Trypanosoma brucei Relies on Malic Enzyme and the Pentose Phosphate Pathway Fed by Gluconeogenic Flux

Stefan Allmann, Pauline Morand, Charles Ebikeme, Lara Gales, Marc Biran, Jane Hubert, Ana Brennand, Muriel Mazet, Jean-Michel Franconi, Paul A. M. Michels, et al.

THE JOURNAL OF BIOLOGICAL CHEMISTRY VOL. 288, NO. 25, pp. 18494–18505, June 21, 2013

Cytosolic NADPH Homeostasis in Glucose-starved Procyclic *Trypanosoma brucei* Relies on Malic Enzyme and the Pentose Phosphate Pathway Fed by Gluconeogenic Flux*[S]

Received for publication, February 19, 2013, and in revised form, May 4, 2013 Published, JBC Papers in Press, May 10, 2013, DOI 10.1074/jbc.M113.462978

Stefan Allmann[‡], Pauline Morand[§], Charles Ebikeme[§], Lara Gales[¶‖], Marc Biran[§], Jane Hubert[¶‖**], Ana Brennand[‡], Muriel Mazet[§], Jean-Michel Franconi[§], Paul A. M. Michels[‡‡], Jean-Charles Portais[¶‖**1], Michael Boshart[‡1,2], and Frédéric Bringaud[§1,3]**

*From the [‡]Faculty of Biology, Section of Genetics, Ludwig-Maximilians-Universität München, Biozentrum, Grosshadernerstrasse 2-4, D-82152 Martinsried, Germany, the [§]Centre de Résonance Magnétique des Systèmes Biologiques (RMSB), UMR5536, Université Bordeaux Segalen, CNRS, 146 rue Léo Saignat, 33076 Bordeaux, France, the [¶]Université de Toulouse, INSA, UPS, INP, LISBP, 135 Avenue de Rangueil, F-31077 Toulouse, France, the [‖]INRA, UMR792 Ingénierie des Systèmes Biologiques et des Procédés, F-31400 Toulouse, France, the **CNRS, UMR5504, F-31400 Toulouse, France, and the [‡‡]Research Unit for Tropical Diseases, de Duve Institute and Laboratory of Biochemistry, Université catholique de Louvain, Avenue Hippocrate 74, B-1200 Brussels, Belgium*

Background: NADPH production is critical for growth and oxidative stress management.
Results: Redundancy of the pentose phosphate pathway and the cytosolic malic enzyme for NADPH synthesis is carbon source-independent in procyclic trypanosomes.
Conclusion: The parasite has gluconeogenic capacity from proline.
Significance: This work illustrates the flexible carbon source-dependent flux changes for essential NADPH supply.

All living organisms depend on NADPH production to feed essential biosyntheses and for oxidative stress defense. Protozoan parasites such as the sleeping sickness pathogen *Trypanosoma brucei* adapt to different host environments, carbon sources, and oxidative stresses during their infectious life cycle. The procyclic stage develops in the midgut of the tsetse insect vector, where they rely on proline as carbon source, although they prefer glucose when grown in rich media. Here, we investigate the flexible and carbon source-dependent use of NADPH synthesis pathways in the cytosol of the procyclic stage. The *T. brucei* genome encodes two cytosolic NADPH-producing pathways, the pentose phosphate pathway (PPP) and the NADP-dependent malic enzyme (MEc). Reverse genetic blocking of those pathways and a specific inhibitor (dehydroepiandrosterone) of glucose-6-phosphate dehydrogenase together established redundancy with respect to H_2O_2 stress management and parasite growth. Blocking both pathways resulted in ~10-fold increase of susceptibility to H_2O_2 stress and cell death. Unexpectedly, the same pathway redundancy was observed in glucose-rich and glucose-depleted conditions, suggesting that gluconeogenesis can feed the PPP to provide NADPH. This was confirmed by (*i*) a lethal phenotype of RNAi-mediated depletion of glucose-6-phosphate isomerase (PGI) in the glucose-depleted Δ*mec*/Δ*mec* null background, (*ii*) an ~10-fold increase of susceptibility to H_2O_2 stress observed for the Δ*mec*/Δ*mec*/^{RNAi}PGI double mutant when compared with the single mutants, and (*iii*) the ^{13}C enrichment of glycolytic and PPP intermediates from cells incubated with [U-^{13}C]proline, in the absence of glucose. Gluconeogenesis-supported NADPH supply may also be important for nucleotide and glycoconjugate syntheses in the insect host.

In any living organism, the cellular redox homeostasis has to be maintained. Reactive oxygen species (ROS)[4] originate from aerobic metabolism or from the environment. ROS include superoxide anions, hydrogen peroxide, and hydroxyl radicals that damage nucleic acids, proteins, lipids, and membranes. Aerobic organisms have evolved efficient antioxidant systems to preserve a reducing milieu. This is particularly true for parasites, which can successfully withstand the oxidative burst that is part of the mammalian host innate immunity upon infection. Reactive oxygen stress conditions are also faced in the fly vector along the digenetic life cycle (1). Many parasitic organisms are highly sensitive to oxidative stress, as observed for the intracel-

* This work was supported by the Agence Nationale de la Recherche (ANR) through Grants METABOTRYP of the ANR-MIME2007 call and ACETOTRYP of the ANR-BLANC-2010 call (to F. B, J. C. P., and M. Boshart) and DFG Grant Bo1100/6–2 (to M. Boshart).
[S] This article contains supplemental Table S1.
[1] Supported by a research cooperation grant of the Franco-Bavarian University Cooperation Center (BFHZ/CCUFB).
[2] To whom correspondence may be addressed. Tel.: 49-89-2180-74600; Fax: 49-89-2180-74629; E-mail: boshart@lmu.de.
[3] Supported by the CNRS, the Université Bordeaux Segalen, the Conseil Régional d'Aquitaine, the Laboratoire d'Excellence (LabEx) ParaFrap ANR-11-LABX-0024, and the ParaMet Ph.D. programme of Marie Curie Initial Training Network (FP7). To whom correspondence may be addressed. Tel.: 33-5-57-57-46-32; Fax: 33-5-57-57-45-56; E-mail: bringaud@rmsb.u-bordeaux2.fr.

[4] The abbreviations used are: ROS, reactive oxygen species; DHEA, dehydroepiandrosterone; F6P, fructose 6-phosphate; FBP, fructose 1,6-bisphosphate; G6P, glucose 6-phosphate; G6PDH, glucose-6-phosphate dehydrogenase; PGI, phosphoglucose isomerase; GOX, glucose oxidase; ME, malic enzyme; MEc, cytosolic NADP-dependent malic enzyme; MEm, mitochondrial NADP-dependent malic enzyme; PEP, phosphoenolpyruvate; PEPCK, phosphoenolpyruvate carboxykinase; PPDK, pyruvate phosphate dikinase; PPP, pentose phosphate pathway; TRYP2, mitochondrial trypanothione-dependent tryparedoxin peroxidase; XOX, xanthine oxidase; MRM, multiple reaction monitoring; IC-MS/MS, ionic-exchange chromatography coupled with tandem mass spectrometry.

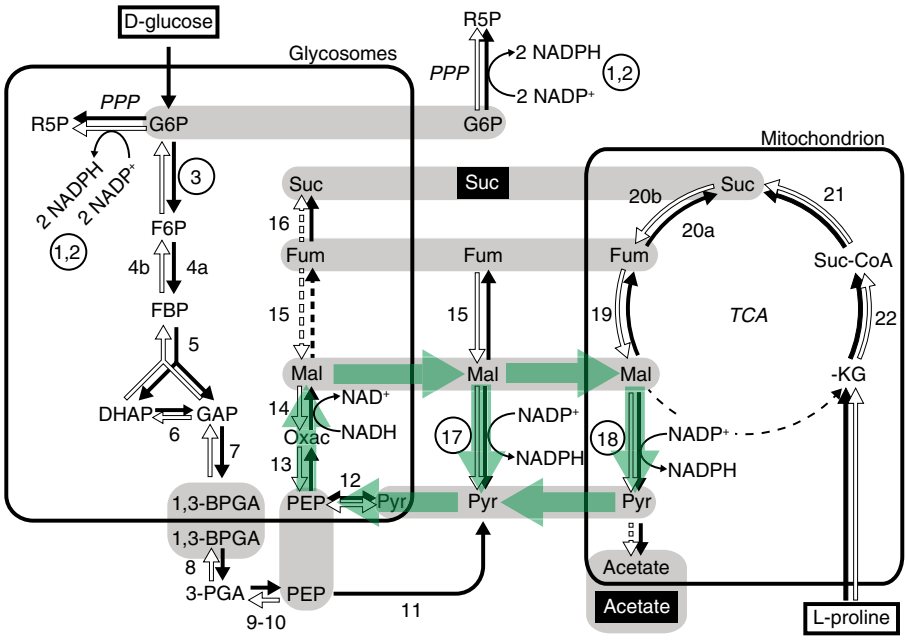

FIGURE 1. **Metabolic network related to NADPH production.** *Black arrows* indicate enzymatic steps of glucose and proline metabolism of procyclic trypanosomes grown in glucose-rich conditions, whereas *white arrows* correspond to proline metabolism in the absence of glucose (66). *Dashed arrows* symbolize steps for which no evidence of flux is available. The proposed NADH/NADPH converting cycle or transhydrogenase-like shunt is indicated by *green arrows*. For simplification, only $NADP^+$/NADPH and NAD^+/NADH involved in the putative transhydrogenase-like shunt are shown. Excreted end products of glucose and proline metabolism are indicated by a *black background*. The pools of metabolites shared by different subcellular compartments are indicated by *gray areas*. Experimental evidence for most of the intracellular transmembrane translocation is missing. The abbreviations used are: *α-KG*, α-ketoglutarate; *1,3-BPGA*, 1,3-bisphosphoglycerate; *3-PGA*, 3-phosphoglycerate; *DHAP*, dihydroxyacetone phosphate; *Fum*, fumarate; *GAP*, glyceraldehyde 3-phosphate; *Mal*, malate; *Oxac*, oxaloacetate; *Pyr*, pyruvate; *R5P*, ribulose 5-phosphate; *Suc*, succinate; *Suc-CoA*, succinyl-CoA. Key enzymes are: **1**, glucose-6-phosphate dehydrogenase; **2**, 6-phosphogluconate dehydrogenase; **3**, glucose-6-phosphate isomerase; **4a**, phosphofructokinase; **4b**, fructose-1,6-bisphosphatase; **5**, aldolase; **6**, triose phosphate isomerase; **7**, glyceraldehyde-3-phosphate dehydrogenase; **8**, cytosolic phosphoglycerate kinase; **9**, phosphoglycerate mutase; **10**, enolase; **11**, pyruvate kinase; **12**, pyruvate phosphate dikinase; **13**, phosphoenolpyruvate carboxykinase; **14**, glycosomal malate dehydrogenase; **15**, cytosolic and glycosomal fumarase; **16**, glycosomal NADH-dependent fumarate reductase; **17**, cytosolic malic enzyme; **18**, mitochondrial malic enzyme; **19**, mitochondrial fumarase; **20a**, mitochondrial NADH-dependent fumarate reductase; **20b**, succinate dehydrogenase; **21**, succinyl-CoA synthetase; **22**, α-ketoglutarate dehydrogenase.

lular stages of *Plasmodium* (2), *Toxoplasma* (3), and *Trypanosoma cruzi* (4) and for extracellular stages such as the *Trypanosoma brucei* bloodstream form (5). Consequently, selective disruption of the parasite redox balance is an effective approach to therapeutic intervention (6–8).

For ROS detoxification in *T. brucei*, electrons from NADPH are transferred through a cascade of electron carriers involving trypanothione and several small dithiol redox proteins (9). Trypanothione is a condensation product of two glutathione molecules and one spermidine molecule (10). Maintenance of the trypanothione-based redox homeostasis is also critical for production of deoxyribonucleotides required for replication and repair of DNA and for metabolism and biogenesis of iron-sulfur clusters. Consequently, interfering with trypanothione biosynthesis and utilization is detrimental for trypanosomes (11–14).

NADPH is the key metabolite in these processes because it is the only source of electrons for trypanothione reduction. NADPH is the product of two enzymatic reactions of the pentose phosphate pathway (PPP), the glucose-6-phosphate dehydrogenase (G6PDH)- and 6-phosphogluconate dehydrogenase-catalyzed steps. Both enzymes show a dual cytosolic and glycosomal localization in trypanosomes (15–18). The oxidative branch of the PPP produces ribose 5-phosphate required for nucleic acid biosynthesis, and NADPH is a major source of reducing equivalents for biosynthetic processes, including *de novo* synthesis of fatty acids (19). Therefore, PPP activity should be essential for the bloodstream form of *T. brucei*, independently of trypanothione metabolism. In fact, in bloodstream, *T. brucei* cell death results from RNAi down-regulation of G6PDH or 6-phosphogluconate dehydrogenase, and incubation with dehydroepiandrosterone (DHEA), a potent uncompetitive inhibitor of G6PDH (20, 21).

The central energy metabolism of the procyclic insect stage is more flexible and can adapt to changing carbon sources. In the midgut, this is mainly proline. For example, NADPH can theoretically be produced in the cytosol and the mitochondrion of the trypanosomatids by two isoforms of the malic enzyme (ME (Fig. 1)) (22). The relative roles of the PPP and alternative reactions to provide NADPH have not been investigated so far.

Here, we show that the oxidative branch of the PPP and the cytosolic MEc isoform can both contribute to and individually sustain the essential NADPH supply in the cytosol of procyclic trypanosomes. Surprisingly, the PPP can also operate in glucose-depleted conditions. We provide direct genetic and metabolomic evidence that this is due to gluconeogenic flux by producing glucose 6-phosphate from proline, illustrating the flexible carbon source-dependent flux changes in the procyclic stage of the parasite.

EXPERIMENTAL PROCEDURES

Trypanosomes and Cell Cultures—The procyclic form of *T. brucei* EATRO1125 was cultured at 27 °C in SDM79 medium containing 10% (v/v) heat-inactivated fetal calf serum and 35

μg/ml hemin (23). The SDM79 used for glucose-depleted growth was modified by omitting glucose and the addition of 50 mM *N*-acetylglucosamine (GlcNAc), which is a nonmetabolized glucose analog inhibiting glucose import (24).

Inhibition of Gene Expression by RNAi—The inhibition by RNAi of gene expression in procyclic forms (25) was performed by expression of stem-loop "sense/antisense" RNA molecules of the targeted sequences (26) introduced in the pLew100 expression vector, which contains the phleomycin resistance gene (kindly provided by E. Wirtz and G. Cross) (27). Construction of the pLew-MEc/m-SAS plasmid used to simultaneously target by RNAi the mRNAs of both malic enzyme genes, which encode the cytosolic and mitochondrial isoforms (*MEc*: *Tb11.02.3120* and *MEm*: *Tb11.02.3130*, respectively) (^{RNAi}MEc/m-C3 cell line), was described before (28). The pLew-MEc-SAS and pLewMEm-SAS plasmids, designed to inhibit by RNAi the expression of the *MEc* gene or the *MEm* gene, respectively, were created in the pLew100 vector with the same strategy described above, employing the same restriction sites. The targeting cassettes correspond to the end of the *MEc* (from position 1465 bp to 1695 bp) or *MEm* (from position 1476 bp to 1716 bp) coding sequence followed by the first 224 or 268 bp, respectively, of the 3′-UTR. The resulting plasmids (pLew-MEc-SAS and pLew-MEm-SAS) contain a sense and antisense version of the targeted gene fragment, separated by a 60- or 40-bp fragment, respectively. The pLew-PGI-SAS plasmid designed to inhibit the expression of the glucose-6-phosphate isomerase (PGI) gene (Tb927.1.3830) was made using the pLew100 vector with the same strategy described above, employing the same restriction sites. The targeting area corresponds to the midsection of the coding region (from position 889 bp to position 1366 bp) of the *PGI* gene. The constructed plasmid (pLew-PGI-SAS) contains a sense and antisense version of the targeted gene area, separated by a 40-bp fragment. The sense-antisense cassette designed to target expression of the *G6PDH* gene (21) was introduced into the HindIII and BamHI sites of the pLew100 vector to produce the pLewG6PDH-SAS plasmid.

Gene Knock-out of the MEc Gene—Replacement of both alleles of the *MEc* gene by the blasticidin and puromycin resistance markers via homologous recombination was performed with DNA fragments containing a resistance marker gene flanked by the *MEc* UTR sequences. Briefly, the pGEMt plasmid was used to clone an HpaI DNA fragment containing the blasticidin (*BSD*) and puromycin (*PAC*) resistance marker gene preceded by the *MEc* 5′-UTR fragment (581 bp) and followed by the *MEc* 3′-UTR fragment (579 bp).

Trypanosome Transfection—The EATRO1125 procyclic form cell line (EATRO1125.T7T), constitutively expressing the T7 RNA polymerase gene and the tetracycline repressor under the control of a T7 RNA polymerase promoter for tetracycline-inducible expression (26), was the recipient of all transfections. Transfection and selection in SDM79 medium containing combinations of hygromycin B (25 μg/ml), neomycin (10 μg/ml), blasticidin (10 μg/ml), phleomycin (5 μg/ml), and puromycin (1 μg/ml) followed previous studies (29). The selected Δ*mec*::BSD/Δ*mec*::PAC cell line (named Δ*mec*), was also transfected with the pLewG6PDH-SAS plasmid to create the Δ*mec*/^{RNAi}G6PDH mutant and the pLew-PGI-SAS plasmid to generate the Δ*mec*/^{RNAi}PGI mutant. The ^{RNAi}PGI mutant was obtained by transfecting the pLew-PGI-SAS plasmid into EATRO1125.T7T. Primer sequences are available upon request.

Enzymatic Assays—Sonicated (5 s at 4 °C) crude extracts of trypanosomes resuspended in cold hypotonic buffer (10 mM potassium phosphate, pH 7.8) were tested for malic enzyme (EC 1.1.1.40) and pyruvate kinase (EC 2.7.1.40) activities (30).

Western Blot Analyses—Total protein extracts of the procyclic form of *T. brucei* (2×10^6 cells) were separated by SDS-PAGE (10%) and blotted on Immobilon-P filters (Millipore) (31). Immunodetection was performed as described (31, 32) using as primary antibodies the rabbit anti-serum against G6PDH (1:1,000 dilution), the mouse anti-serum against the cytosolic fumarase (1:100 dilution) (33), and the mouse anti-serum against the mitochondrial trypanothione-dependent tryparedoxin peroxidase (TRYP2) (1:500 dilution) (34). Goat anti-rabbit or anti-mouse Ig/peroxidase (1:10,000 dilution) was used as secondary antibody, and enzyme activity was revealed using ECL™ Western blotting detection reagents as described by the manufacturer (Amersham Biosciences). For Western blot analyses of the PGI protein, an Immobilon-FL membrane (Millipore) was used along with infrared fluorescence detection by the Odyssey scanner (LI-COR). The polyclonal rabbit anti-serum against the PGI (1:800) was detected by the goat anti-rabbit antibody IRDye680LT (1:25,000) (LI-COR). The monoclonal paraflagellar rod mouse anti-serum L13D6 (1:2,000) (35) was detected with the goat anti-mouse IRDye800 (1:10,000) (LI-COR).

Oxidative Stress Assays—The susceptibility of trypanosomes toward oxidative stress was measured with an adapted protocol of the Alamar Blue assay (36, 37). Cells were grown to densities between 6×10^6 and 1.5×10^7 cells/ml and diluted to 4×10^6 cells/ml (glucose oxidase (GOX) assays) or 1.5×10^6 cells/ml (xanthine oxidase (XOX) assays). A volume of 180 μl of cell suspension was distributed to the corresponding wells of a 96-well plate. Then 20 μl of GOX or XOX solutions with increasing concentrations were added to the respective wells (GOX and XOX from Sigma). After a 22-h (GOX) or 44-h (XOX) incubation, 20 μl of a 0.49 mM resazurin (Sigma) solution in PBS were added to each well, and 2 h later, the fluorescence was measured in a Tecan Safire plate reader with an excitation wavelength of 530 nm and an emission wavelength of 590 nm. The background caused by the medium was measured and subtracted. All Alamar Blue assay results are mean of triplicate assays of a given biological experiment. Wells without the addition of GOX/XOX were used as reference and set to 100% cell viability. When using XOX as inducing agent, 5 mM hypoxanthine was added to the culture medium as substrate. The G6PDH inhibitor DHEA was added to the respective cultures at 15 μM 24 h before inducing oxidative stress.

Mass Spectrometry Analysis—Wild-type cells grown in glucose-rich or glucose-depleted medium were washed twice with PBS and resuspended in PBS containing 2 mM [U-^{13}C]proline with (10 mM) or without glucose, respectively. The cells were incubated for 2 h at 27 °C before fast filtration preparation of the samples for mass spectrometry analysis, as described before

TABLE 1

Detection parameters for quantitative analysis of intracellular metabolites by IC-MS/MS

The analysis was performed by ion-exchange chromatography coupled to triple-quadrupole-mass spectrometry in the MRM mode. 2-PGA, 2-phosphoglycerate; 3-PGA, 3-phosphoglycerate; 1,3-BPGA, 1,3-bisphosphoglycerate.

Metabolites	Formula	M_r	Retention time[a]	[M-H]-	MRM transition[b]	MRM transition U-^{13}C[c]
		$g \times mol^{-1}$	*min*			
PEP	$C_3H_5O_6P$	167,982	38.2	166,975	167/79	170/79
2-PGA	$C_3H_7O_7P$	185,993	33.6	184,986	185/97	188/97
3-PGA	$C_3H_7O_7P$	185,993	33.6	184,986	185/97	188/97
1,3-BPGA	$C_3H_8O_{10}P_2$	265,959	38.0	264,952	265/79	268/79
FBP	$C_6H_{14}O_{12}P_2$	339,996	48.6	338,989	339/97	345/97
F6P	$C_6H_{13}O_9P$	260,030	20.3	259,022	259/97	265/97
G6P	$C_6H_{13}O_9P$	260,030	19.2	259,022	259/97	265/97
6PG	$C_6H_{13}O_{10}P$	276,025	31.4	275,017	275/97	281/97
S7P	$C_7H_{15}O_{10}P$	290,040	24.0	289,030	289/97	296/97

[a] The molecular information, chromatographic retention times.
[b] MRM transitions for the analyzed metabolites.
[c] MRM transitions of the [^{13}C-U]-labeled compounds used as internal standards.

(38). Metabolites were analyzed by ionic-exchange chromatography coupled with tandem mass spectrometry (IC-MS/MS) using the method described by Bolten *et al.* (39). Retention time on the column and multiple reaction monitoring (MRM) transition of each analyzed metabolite are shown in Table 1. The ^{13}C mass isotopomer distribution of intracellular metabolites was determined from relevant isotopic clusters in the IC-MS/MS analysis, according to Kiefer *et al.* (40). ^{13}C mass isotopomer distribution measurements were performed using a triple quadrupole mass spectrometer (4000Qtrap, Applied Biosystems). To obtain ^{13}C-labeling patterns (^{13}C isotopologues), isotopic clusters were corrected for the natural abundance of isotopes other than ^{13}C, using the in-house software IsoCor (available at MetaSys) (41).

RESULTS

Subcellular Localization of the ME Activity in Procyclic T. brucei—In procyclic trypanosomes grown in glucose as carbon source, the PPP is a major source of NADPH (15). However, other NADP-dependent enzymatic activities, such as that of ME, have been reported in insect stage trypanosomatids (42, 43). Two isoforms of the NADP-dependent ME are encoded in the *T. brucei* genome, MEc (Tb11.02.3120) and MEm (Tb11.02.3130), and they might contribute to NADPH regeneration. One isoform (MEm) has a potential N-terminal mitochondrial targeting sequence (0.90 probability MITOPROT prediction). To address the subcellular localization of the ME activity, procyclic *T. brucei* cells were permeabilized with increasing concentrations of digitonin. Soluble and insoluble fractions at each concentration were separated and analyzed for ME activity (Fig. 2*A*). A mitochondrial marker (TRYP2) and a cytosolic marker (cytosolic fumarase) were quantified by Western analysis of an aliquot of each fraction (Fig. 2*B*). ME activity is released to the supernatant at low digitonin concentrations, which correlates with the cytosolic marker. A second release of activity to the supernatant at higher digitonin concentration correlates with the appearance of the mitochondrial marker. In summary, ME activity is dually localized and equally distributed among the cytosolic and mitochondrial compartments.

Analysis of ME-deficient Cell Lines—To investigate the respective functional roles of the isoforms, we created three different inducible RNAi knockdown cell lines. One RNAi hairpin construct targets both ME isoforms (^{RNAi}MEc/m), and the other constructs each target specifically the individual isoforms (^{RNAi}MEc or ^{RNAi}MEm). RNAi against both isoforms led to a severe growth phenotype 4 days after induction with tetracycline (Fig. 3*A*). Samples were taken in parallel for ME activity assays. The ME activity is decreased to a very low level after 3–4 days, correlating with the growth phenotype (Fig. 3*A*). In the RNAi cell lines targeting only the cytosolic ME, we did not see a growth phenotype (Fig. 3*C*), but targeting the mitochondrial isoform resulted in the severe phenotype (Fig. 3*B*), similar to that observed when targeting both isoforms (Fig. 3*A*). All non-induced clones showed normal growth (Fig. 3, *A*–*C*). The ME activities were reduced to ~40% after tetracycline induction in the cell lines with singly targeted MEc or MEm (Fig. 3, *B* and *C*). We concluded that under standard culture conditions, the

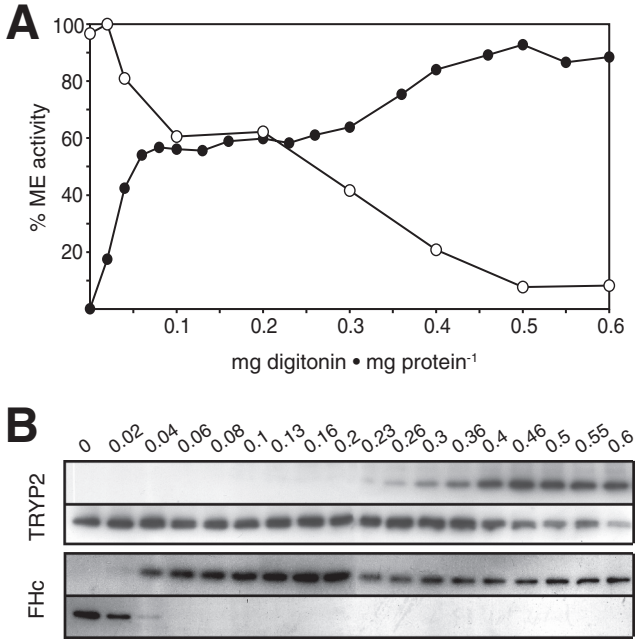

FIGURE 2. **Subcellular localization of ME activity by digitonin titration in procyclic *T. brucei*.** *A*, the ME activity was determined in the supernatant (*filled circle*) and pellet (*open circle*) fractions from cells incubated with 0.02–0.6 mg of digitonin/mg of protein in STE buffer (250 mM sucrose, 25 mM Tris-HCl, pH 7.4, 1 mM EDTA) containing 150 mM NaCl, as indicated. *B* shows a Western blot analysis of marker proteins in the same supernatant (*S*) and pellet (*P*) fractions: mitochondrial trypanothione-dependent tryparedoxin peroxidase (*TRYP2*) and cytosolic fumarate hydratase (*FHc*).

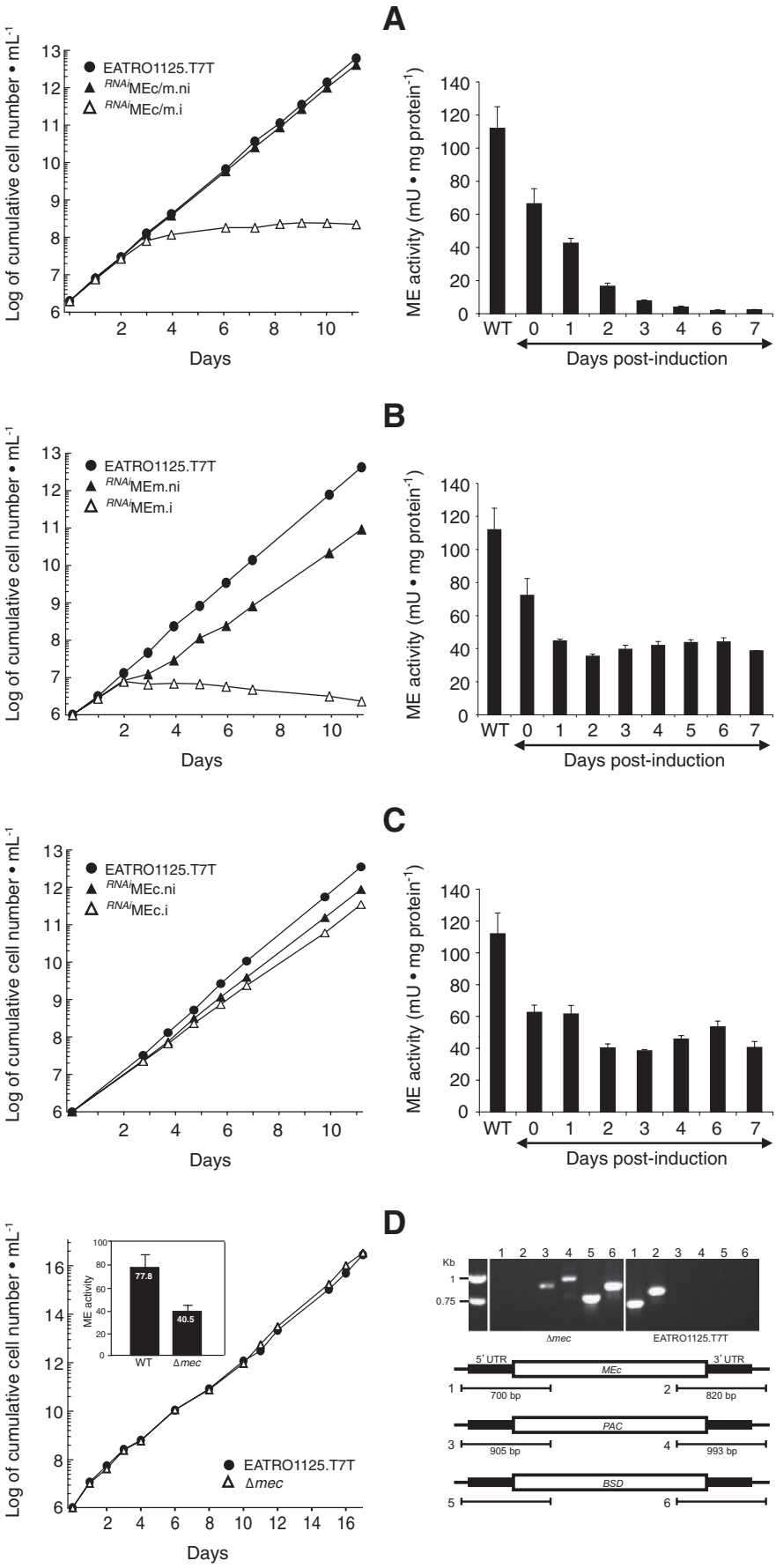

mitochondrial ME isoform is essential, but not the cytosolic ME. This was fully confirmed by the successful creation of a Δ*mec*/Δ*mec* knock-out cell line, named Δ*mec* (Fig. 3*D*). As expected, this line proliferated as the parental control, and the remaining total ME activity within the Δ*mec* line was similar to the activity in the induced ^{RNAi}MEc line (Fig. 3*D*).

Cytosolic ME-deficient (Δmec) Cells Cannot Tolerate Depletion or Inhibition of G6PDH—To explore an alternative source of NADPH of possible physiological relevance in procyclic *T. brucei*, we depleted the major NADPH source, the PPP in the wild-type background and in the Δ*mec* mutant background. There are two NADPH-producing steps in the PPP, G6PDH and 6-phosphogluconate dehydrogenase. By depleting or inhibiting G6PDH, the downstream 6-phosphogluconate dehydrogenase activity is also affected due to substrate limitation. Knockdown of *G6PDH* by RNAi in the wild-type background had no effect on the growth of the cells (Fig. 4*A*), in contrast to the same treatment in the bloodstream stage (20, 21). However, the induction of the *G6PDH* RNAi in the Δ*mec* background resulted in one of the most dramatic growth phenotypes we observed so far in procyclic trypanosomes (Fig. 4*B*). As *MEc* can rescue the *G6PDH* deficiency, the main function of the *MEc* is obviously NADPH production. We also conclude that the degree of RNAi-mediated repression of G6PDH is limiting for NADPH production but not for ribose synthesis. The genetic interaction was confirmed by chemical inhibition of *T. brucei* G6PDH by DHEA, a specific inhibitor of G6PDH in *T. brucei* (20, 21, 44). We determined the LD_{50} of this compound for the procyclic Δ*mec* line to be 18 μM after 48 h of incubation (Fig. 4*D*). The LD_{50} for wild-type cells was at least 10-fold higher (data not shown). Using 15 μM DHEA, we observed a growth defect and cell death after 5–6 days in Δ*mec* cells but not in wild-type cells, exactly as upon RNAi induction (Fig. 4*C*). The IC_{50} value for G6PDH inhibition by DHEA *in vitro* is 2.8 ± 0.6 μM (44). Assuming efficient uptake of the drug, 15 μM DHEA would result in 86% inhibition of G6PDH. As wild-type cells can perfectly tolerate much higher concentrations of DHEA (not shown) as well as efficient RNAi depletion of G6PDH (Fig. 4*A*), we attempted to delete the *G6PDH* gene. Although we obtained double drug-resistant lines with *G6PDH* locus-specific marker integration, a *G6PDH* allele or G6PDH protein was always retained in these clones, suggestive of triploidization (supplemental Table S1). In trypanosomes, this type of locus triploidization upon targeting is indicative of gene essentiality (45), which can be also observed in *Leishmania* (46). We concluded that *G6PDH* and *ME* are redundant with respect to NADPH production, yet the PPP must have an additional and essential function. The cells might well tolerate PPP deficiency over the short time of RNAi-dependent knockdown or DHEA inhibition experiments, but for clonal outgrowth of cells, the PPP seems to be essential, probably because of its function in nucleotide synthesis (47, 48).

Δ*mec Mutant Cells Control Oxidative Stress in the Absence of Glucose*—As a sensitive assay for the contributions of *G6PDH* and *MEc* to NADPH production, we quantified the oxidative stress sensitivity of the respective mutants. Detoxification of ROS depends on NADPH supply. Oxidative stress was applied by continuous H_2O_2 production with GOX or XOX in the growth medium (49, 50). This results in a more physiological stress type when compared with the bolus application of H_2O_2, which acts only transiently with a half-life time of about 10 min under standard culture conditions (51). DHEA-mediated inhibition of G6PDH or deletion of *MEc* alone resulted in a very moderate increase in susceptibility (Fig. 5*A*). However, incubation of the Δ*mec* mutant cell line with 15 μM DHEA for 2 days caused a severe increase in H_2O_2 susceptibility (Fig. 5*A*) and growth inhibition (Fig. 4*D*). These data confirm the redundancy of the PPP and the MEc activities for NADPH production and for maintenance of the cytosolic redox state when glucose is available as carbon source.

Procyclic trypanosomes grow in essentially glucose-free conditions in the insect gut. Therefore, we tested the Δ*mec* mutant in glucose-depleted medium for susceptibility to oxidative stress. We expected increased susceptibility due to low PPP activity under glucose-depleted conditions. Fig. 5*B* shows that the Δ*mec* mutant was not significantly more susceptible to oxidative stress than wild-type cells. By inhibition of G6PDH (and hence the PPP) with DHEA, we obtained the same phenotype as in glucose-fed conditions. One possible explanation would be that uptake of residual glucose from the serum is sufficient to feed the PPP. This is, however, extremely unlikely as we added a large excess of GlcNAc (50 mM) to the medium to inhibit the uptake of the residual glucose present in FCS (0.5 mM). GlcNAc has been shown to inhibit glucose-uptake (24). The alternative would be glucose-independent supply of glucose 6-phosphate (G6P) via gluconeogenic flux. Production of glucose 6-phosphate from a non-glycolytic source through gluconeogenesis has been suspected in trypanosomatids but not experimentally verified to date (52).

Inhibition of Glucose-independent G6P Production Phenocopies G6PDH Deficiency—To address the possibility of glucose-independent supply of G6P, expression of the *PGI* gene was down-regulated by RNAi in the wild-type and the Δ*mec* mutant background. PGI and hexokinase are the only enzymes in *T. brucei* that can give rise to G6P as product (Fig. 1). Therefore, in glucose-depleted medium, the tetracycline-induced Δ*mec*/^{RNAi}PGI double mutant but not the single ^{RNAi}PGI mutant should phenocopy the combined *MEc* and *G6PDH* deficiency. The growth behavior of the respective cell lines in glucose-rich and glucose-depleted conditions is shown in Fig. 6.

FIGURE 3. **Growth of ME-deficient cell lines.** *A–D*, growth curves of ^{RNAi}MEc/m (*A*), ^{RNAi}MEm (*B*), ^{RNAi}MEc (*C*), and Δ*mec* (*D*) mutants. The parental cell line (EATRO1125.T7T) was included in each experiment. Cells were maintained in the exponential growth phase (between 10^6 and 10^7 cells/ml) by dilution, and cumulative cell numbers are presented with and without tetracycline-dependent induction as indicated. Malic enzyme activities of induced RNAi mutants (*A–C*) and of the Δ*mec* mutant (*D*) are shown together with the parental cells on the *right-hand graph* or as an *inset* in the growth curve, respectively. *Error bars* indicate the S.D. of three independent experiments. *D* also shows a PCR analysis of genomic DNA isolated from the parental EATRO1125.T7T (*WT*) and Δ*mec* cell lines to confirm *MEc* gene deletion. The *lower panel* shows PCR fragments amplified with primers based on sequences that flank the 5′-UTR and 3′-UTR fragments used to target the *MEc* gene disruption (*black boxes*) and internal sequences from the *MEc* gene (PCR products 1 and 2), the puromycin resistance gene (*PAC*, PCR products 3 and 4) or the blasticidin resistance gene (*BSD*, PCR products 5 and 6). *mU,* milliunits; *μU,* microunits.

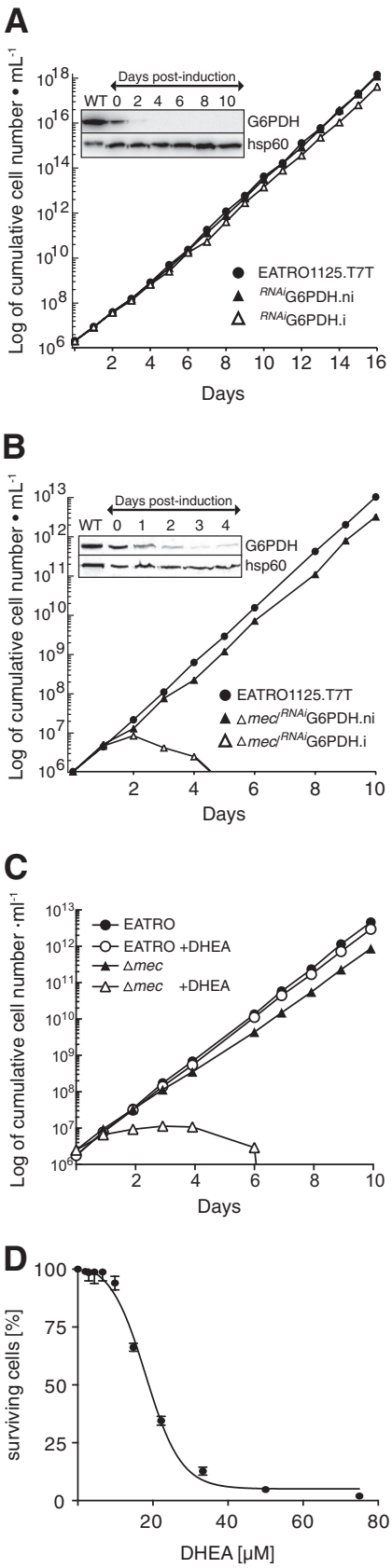

FIGURE 4. **Cells deficient in cytosolic ME (Δ*mec*) cannot tolerate depletion or inhibition of G6PDH in glucose rich-conditions.** *A* and *B*, RNAi-mediated down-regulation of G6PDH in the wild-type (*WT*) (*A*) or Δ*mec* background (*B*). The control of RNAi efficiency by Western blot analysis is shown as the *inset*. *C*, inhibition of G6PDH by a specific inhibitor (DHEA, 15 μM). *D*, dose response curve for DHEA. The estimated LD_{50} for 48-h incubation with DHEA is 18 μM in the Δ*mec* line. The LD_{50} (48 h) of DHEA for the parental EATRO1125.T7T line is >10-fold higher (data not shown). All experiments were performed in growth medium containing glucose. *Error bars* represent the S.E. of four independent experiments.

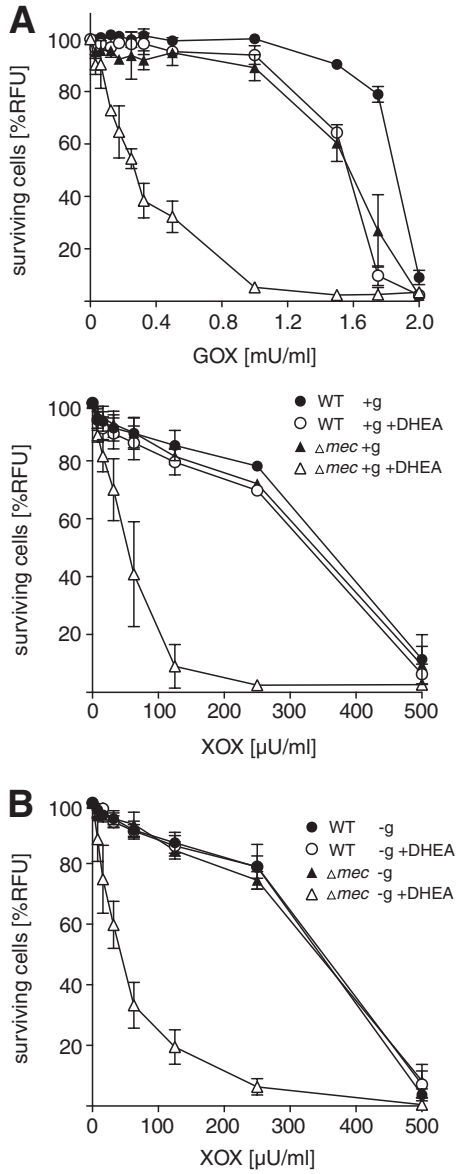

FIGURE 5. **Susceptibility of Δ*mec* mutant cells to oxidative stress.** *A*, induction of oxidative stress by different concentrations of GOX or XOX in glucose-rich medium. *mU*, milliunits. *B*, induction of oxidative stress using XOX in glucose-depleted medium. Cell viability was quantified by the Alamar Blue assay (see "Experimental Procedures"). The relative fluorescence (*%RFU*) was calculated by normalization to the GOX/XOX untreated control for each cell line. *Error bars* represent the S.E. of three independent experiments. μ*U*, microunits.

Under glucose-depleted conditions (Fig. 6*B*), only the induced Δ*mec*/^{RNAi}PGI but not the induced ^{RNAi}PGI mutant died. Thus, cell death is likely to result from NADPH depletion in analogy to the Δ*mec*/^{RNAi}G6PDH double mutant (Fig. 4*B*). Tetracycline induction in the presence of glucose (Fig. 6*A*) resulted in cell death in both the Δ*mec*/^{RNAi}PGI and the ^{RNAi}PGI mutants. This is expected due to glycosomal ATP depletion as glycolysis is blocked. The ATP consumed to produce G6P cannot be

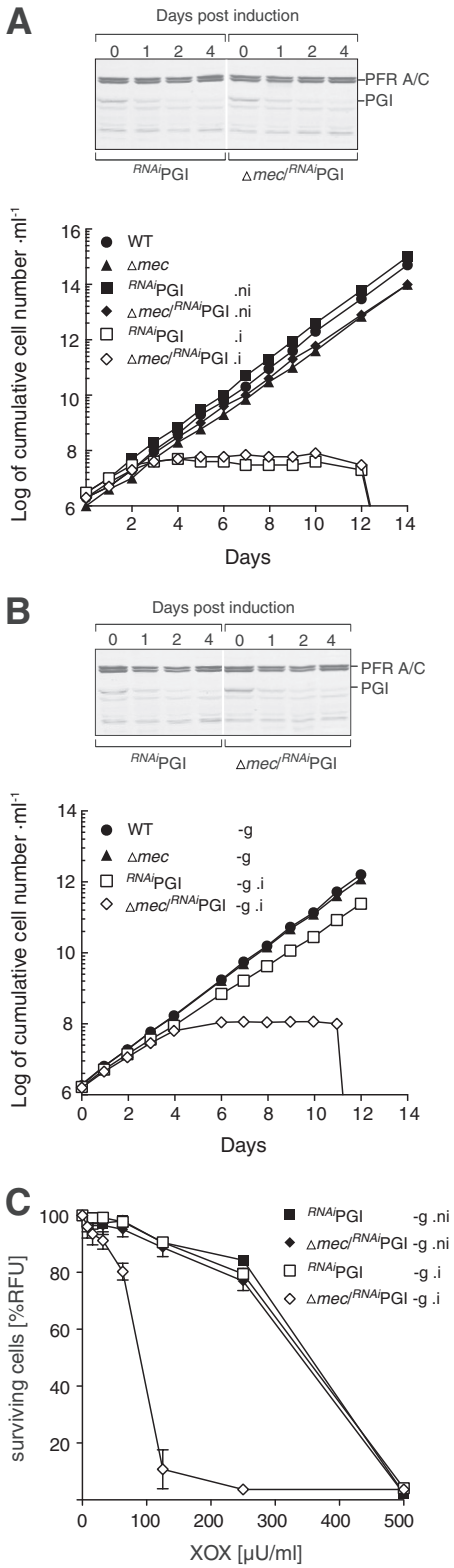

FIGURE 6. **RNAi-mediated depletion of PGI.** *A* and *B*, growth of the wild-type (*WT*), Δ*mec*, ^{RNAi}PGI, and Δ*mec*/^{RNAi}PGI cell lines in glucose-rich (*A*) and glucose-depleted (*B*) medium. The control of RNAi efficiency by Western blot analysis is shown above the growth curves (*PFR A/C*, paraflagellar rod proteins A and C). PGI protein levels after 4 days of induction were quantified as 15 and 13% (*A*) or 10 and 11% (*B*) for the single and double mutants, respectively. *C*, induction of oxidative stress by different concentrations of XOX in glucose-depleted medium. RNAi was induced with tetracycline 72 h prior to addition of XOX. *Error bars* represent the S.E. of three independent experiments.

regained in the pathway. The same mutant cell lines were then subjected to oxidative stress assays in glucose-depleted conditions (Fig. 6*C*). The induced ^{RNAi}PGI mutant showed the same susceptibility as the uninduced control, but the induced Δ*mec*/^{RNAi}PGI had significantly increased oxidative stress susceptibility. It should be noted that the result in Fig. 6*C* is virtually indistinguishable from the analogous experiment with MEc and G6PDH double deficiency (Fig. 4*B*). This further supports the redundant roles of *MEc* and the PPP to provide the essential cytosolic NADPH. Most interestingly, under glucose-depleted culture conditions, the PPP seems clearly active. This reveals gluconeogenic flux up to the level of G6P. In the physiological context, this G6P should derive from proline.

Metabolic Evidence of Gluconeogenesis—To investigate the gluconeogenic flux from proline as carbon source, procyclic cells were incubated with uniformly ^{13}C-enriched proline ([U-^{13}C]proline) in the presence and absence of glucose. Incorporation of ^{13}C into intermediate metabolites was quantified by IC-MS/MS, and the values for selected glycolytic and PPP metabolites are shown in Fig. 7. The incorporation of ^{13}C atoms into glycolytic metabolites in the presence of glucose was low (Fig. 7*A*), as expected, as the proline consumption is repressed by the presence of glucose (53). High ^{13}C incorporation was observed with proline as the only carbon source (Fig. 7*B*). For all glycolytic intermediates analyzed (phosphoenolpyruvate (PEP); 2- or 3-phosphoglycerate (2/3-PGA); 1,3-bisphosphoglycerate (1,3-BGA); fructose 1,6-bisphosphate (FBP); fructose 6-phosphate (F6P), and G6P), the fraction of ^{13}C-enriched molecules is >85% in glucose-depleted conditions when compared with ~10% in the presence of glucose. For additional control, glutamine was added to the medium in glucose-depleted conditions. Glutamine has been shown to serve as carbon source and share with proline the same degradation pathway from glutamate (53). As expected, isotopic dilution was seen (Fig. 7*B*). In contrast, the addition of threonine only resulted in a minimal dilution effect (Fig. 7*B*). Threonine can be degraded to acetyl-CoA but can neither repress proline consumption, as does glucose, nor compete with proline degradation. The relative low amounts of [U-^{13}C]hexose phosphate (FBP, F6P, and G6P) and [U-^{13}C]triose phosphate glycolytic intermediates when compared with partially ^{13}C-enriched molecules (Fig. 7*A*) are probably due to introduction of ^{12}C carbons at the carboxylation/decarboxylation step catalyzed by PEP carboxykinase (PEPCK) and the complete reversibility of the PEPCK/malate dehydrogenase/fumarase branch (54).[5]

The key result of this experiment is the evidence for production of [U-^{13}C]G6P from [U-^{13}C]proline. As this occurs only in glucose-depleted conditions, clear evidence for flux in the gluconeogenic direction is derived. Interestingly, the same degree of enrichment is seen for hexose phosphates (FBP, F6P, and G6P) and the PPP intermediates (6-phosphogluconolactone and sedoheptulose 7-phosphate), confirming that proline-derived G6P feeds the PPP.

[5] J. Hubert, P. Morand, C. Ebikeme, M. Biran, J.-M. Franconi, M. Boshart, J.-C. Portais, and F. Bringaud, unpublished data.

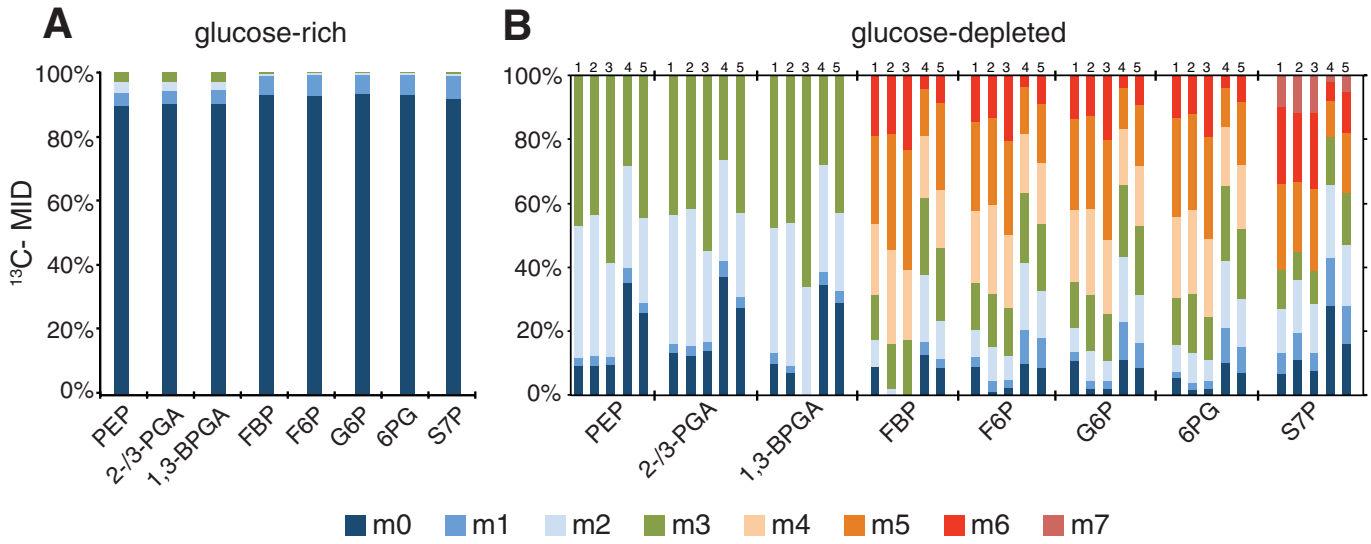

FIGURE 7. **IC-MS/MS analysis of metabolites after isotopic labeling with [U-^{13}C]proline.** EATRO1125.T7T cells were incubated for 2 h in PBS containing 2 mM [U-^{13}C]proline with (*A*) or without (*B*) glucose prior to metabolite extraction. Enrichment at 0–7 carbon positions (*m0* to *m7*) with ^{13}C expressed as the percentage of all corresponding molecules (*MID*; mass isotopomer distribution). 2-Phosphoglycerate and 3-phosphoglycerate are undistinguished by IC-MS/MS and indicated as 2- or 3-phosphoglycerate (*2-/3-PGA*). The other abbreviations used are: *1,3-BPGA*, 1,3-bisphosphoglycerate; *6PG*, 6-phosphogluconate; *S7P*, sedoheptulose 7-phosphate. *B* shows two independent experiments of wild-type cells incubated with 2 mM [U-^{13}C]proline (*lanes 1* and *2*), whereas in *lanes 3–5*, the [U-^{13}C]proline-containing medium was supplemented with threonine (3.4 mM), glutamine (3.5 mM), or both, respectively. For each experiment, triplicate samples have been analyzed by MS with S.E. in the following ranges: PEP, 0.0–1.0%; *2-/3-PGA*, 0.0–1.3%; 1,3-BPGA, 0.0–4.2%; FBP, 0.0–8.0%; F6P, 0.1–4.9%; G6P, 0.0–6.2%; *6PG*, 0.0–2.1%; *S7P*, 0.0–1.8%.

DISCUSSION

Although glucose is sparse or absent in the natural environment of procyclic trypanosomes, the insect midgut (55), the common *in vitro* culture conditions are glucose-rich. Here, we have identified the metabolic pathways used to produce cytosolic NADPH, in glucose-rich and glucose-depleted conditions. The reduced cofactor NADPH is essential for biosynthetic pathways and detoxification of ROS generated by oxidative stress. The candidate enzymatic reactions providing NADPH in the cytosol, *i.e.* the first and third steps of the PPP (G6PDH and 6-phosphogluconate dehydrogenase, respectively) and MEc, were shown to have a redundant function in glucose-rich conditions. The Δ*mec*/^{RNAi}G6PDH.i (where "i" stands for tetracycline-induced) double mutant dies rapidly after a few days of induction, whereas the Δ*mec* and ^{RNAi}G6PDH.i single mutants show no significant growth alteration. Hypersusceptibility to oxidative stress of the Δ*mec* cell line incubated with DHEA, a specific inhibitor of G6PDH, indicates that the common function of the two pathways is production of NADPH, which is essential for defense against ROS. This redundancy may compensate in trypanosomatids for the lack of a transhydrogenase gene (56), which in other organisms catalyzes the reversible conversion of NADH into NADPH. In contrast to procyclic cells, the bloodstream form cells of *T. brucei* are highly susceptible to DHEA (21). This implies that the contribution of MEc to NADPH production is minor in bloodstream trypanosomes, although MEc is expressed in this developmental stage (22). The essential function of the PPP for NADPH production in bloodstream forms is in agreement with the high glycolytic and PPP fluxes, whereas metabolic flux through MEc is expected to be relatively low (15). A low level of PPP function may also be essential upon long term culture of procyclic cells due to the role in nucleotide biosynthesis through ribose 5-phosphate. This is supported by our inability to knock out the *G6PDH* gene.

In contrast to expectation, the PPP and MEc pathways can both provide NADPH to procyclic cells, also in glucose-depleted conditions. As a control, the Δ*mec*/^{RNAi}G6PDH.i double mutant died in glucose-depleted medium (data not shown) as it did in glucose-rich medium (Fig. 4*B*). However, the susceptibility to oxidative stress of the wild-type cells incubated or not with DHEA was the same as the sensitivity of Δ*mec* mutant cells in glucose-depleted conditions. This provided strong evidence for a flux through the PPP in the absence of glucose, suggesting an alternative hexokinase-independent source of G6P. The obvious hypothesis, gluconeogenesis, was confirmed by the observed oxidative stress hypersensitivity of the Δ*mec*/^{RNAi}PGI.i mutant in a glucose-depleted environment. PGI, the enzyme reversibly converting F6P into G6P, is an essential step of gluconeogenesis. In addition to this genetic evidence, we directly demonstrated for the first time *bona fide* gluconeogenesis in *T. brucei* by ~9-fold increase of ^{13}C incorporation into glycolytic and PPP intermediates from [U-^{13}C]proline. Proline is the main available carbon source in the absence of glucose (53). Hannaert and colleagues (52, 57) had proposed gluconeogenic capacity in the glycosomes of *T. brucei* because the genome encodes a glycosomal fructose-1,6-bisphosphatase. However, no experimental evidence of gluconeogenesis has been reported for either procyclic or bloodstream forms of *T. brucei*.

What is the benefit of redundant NADPH sources in procyclic *T. brucei* in both glucose-rich and glucose-depleted conditions? The primary role of the irreversible reaction catalyzed by MEc is apparently cytosolic NADPH production. Therefore, MEc can provide a high flexibility to adapt NADPH production to cellular need, whatever carbon source is available. In glucose-depleted conditions, carbon flow from proline metabolism can

be redistributed toward the MEc route without affecting production of the essential gluconeogenic precursor PEP. Indeed, PEP can be produced from three different pathways starting from cytosolic malate (MEc and the glycosomally located pyruvate phosphate dikinase (PPDK)), mitochondrial malate (MEm and PPDK), or glycosomal malate (malate dehydrogenase and PEPCK) (28). A single route is sufficient to feed gluconeogenesis (Fig. 1, *white arrows*). This redundancy is confirmed by the nearly wild-type growth rates of Δ*mec*, Δ*pepck*, and Δ*ppdk* null mutants (38) (Fig. 6*B* and data not shown). In glucose-rich conditions, the MEc reaction is a single-step bridge between two main branches of glucose metabolism that lead to mitochondrial succinate and acetate production (Fig. 1, *black arrows*). Redistribution of the carbon flow toward acetate production from glucose-derived malate has no significant impact on the growth rate and allows an increase of NADPH production through MEc. Flux reduction in the mitochondrial succinate branch, due to this redistribution, is well tolerated because ablation of this branch by Δ*pepck*, ^{RNAi}FRDm (mitochondrial NADH-dependent fumarate reductase), or ^{RNAi}FHm (mitochondrial fumarase) mutants does not affect the growth rate of procyclic cells (33, 38, 58). Thus, an increase of NADPH demand may lead to an increase of acetate production from glucose metabolism. The suggested role of MEc is consistent with a recent *in silico* analysis of flux distribution between the different metabolic branches using a multiobjective-criteria bioinformatics approach (59). The simulations predict that ME activity is primarily responsible for the high flexibility observed for the excreted succinate/acetate ratio (33, 54).

As an extension of the flux redistribution model discussed above, we propose a cycle able to increase the metabolic flux through MEc in both glucose-depleted and glucose-rich conditions. Given the reversibility of the PPDK reaction (60), a cycle made up of MEc and three glycosomal steps (PPDK working in the gluconeogenic direction, PEPCK, and malate dehydrogenase) may operate without impact on the energy metabolism and glycosomal ATP balance to produce cytosolic NADPH sustained by NADH production in the glycosomes (Fig. 1, *green arrows*). The relevance of this hypothetical cycle, which may also include the mitochondrial MEm instead of MEc, is its ability to substitute for the absence of cytosolic and mitochondrial transhydrogenases. A similar cycle for converting NADH into NADPH has been engineered in *Saccharomyces cerevisiae*, and due to its function, it was named transhydrogenase-like shunt (61). A *S. cerevisiae* strain was modified to optimize ethanol production, which was limited by the redox imbalance created during fermentation. By overexpressing ME, malate dehydrogenase, and pyruvate carboxylase, it was possible to decrease NADH levels by using it for NADPH for the cost of ATP, which is used during the reaction catalyzed by pyruvate carboxylase. The cycle we propose in *T. brucei* is able to use glycosomal NADH for production of cytosolic/mitochondrial NADPH without a net cost of ATP as PPDK and PEPCK replace pyruvate carboxylase (Fig. 1, *green arrows*). The ATP used in the PPDK reaction is regained in the PEPCK reaction. Our proposed transhydrogenase-like shunt is therefore potentially more efficient than the synthetic one used for metabolic engineering of *S. cerevisiae*. The cycle depends on glycosomal NADH availability and may only be active temporarily to compensate peak demands of cytosolic NADPH, *e.g.* during oxidative stress. Irrespective of the precise model, MEc clearly serves to ensure the essential NADPH production in procyclic trypanosomes in different metabolic situations. This may be most relevant in the insect vector, where a relatively low flux through the oxidative branch of the PPP has to be supported by gluconeogenesis.

A second ME isoform (MEm) is expressed in the *T. brucei* mitochondrion and accounts for approximately half of the total ME activity in procyclic cells (Figs. 1 and 2). In contrast to MEc, MEm is essential, whatever carbon source is provided. MEm also builds a single-step bridge between the mitochondrial succinate and acetate pathways and is not critical for the metabolic network. This strongly supports the view that MEm is essential mainly for NADPH production. The argument implies that there is no other significant source of NADPH in the mitochondrion of procyclic cells. The absence of transhydrogenases in trypanosomatids has already been mentioned.

The metabolism of trypanosomes in the tsetse vector or under conditions mimicking the tsetse environment is a largely unexplored field of research and of key interest to understand the developmental adaptations in the life cycle. In this context, our direct demonstration of a gluconeogenic flux is an important advance. Gluconeogenesis seems to be essential for virulence of the related pathogen *Leishmania major* in macrophages and establishment of infection in mice. When intracellular stages that reside in the parasitophorous vacuole cannot support gluconeogenesis (62) or synthesize specific sugars (63), the amastigotes stop replicating but remain viable. This cell cycle arrest phenotype may be caused by depletion of ribulose 5-phosphate for nucleotide synthesis. Supplementation with exogenous amino acids stimulates the growth of intracellular amastigotes (64), suggesting adaptation of the amastigotes to the sugar-poor but amino acid-rich environment. In the gut and hemolymph of the insect vector of *T. brucei*, a gluconeogenic flux may not only contribute to maintain the redox balance of the cell, but be crucial for synthesizing ribulose 5-phosphate and certain sugars for cell surface glycoconjugates, as shown in *Leishmania* (62). As discussed above, NADPH can also be provided by ME as an alternative source. Recent studies on cancer cells demonstrated that ME plays a central metabolic role in controlling NADPH levels and furthermore plays a regulatory role in preventing senescence of mammalian cells (65). The surprising similarity of metabolic adaptation mechanisms to meet NADPH demand in response to growth conditions highlights the importance of investigating metabolism in defined functional states, be it developmental stages of a parasite, host environment, or the proliferative capacity and malignancy of differentiated mammalian cell populations in the tissue context.

Acknowledgments—We are grateful to Larissa Ivanova (Ludwig-Maximilians Universität Munich) and Nicolas Plazolle (Université Bordeaux Segalen) for invaluable technical support. We thank Artur Cordeiro for providing DHEA. The mass spectrometry equipment and nuclear magnetic resonance equipment used in this study are part of the MetaToul platform (Toulouse, France) that is funded by the Région Midi-Pyrénées, the European Regional Development Fund (ERDF), the INRA, and the CNRS, which are gratefully acknowledged.

REFERENCES

1. Hao, Z., Kasumba, I., and Aksoy, S. (2003) Proventriculus (cardia) plays a crucial role in immunity in tsetse fly (Diptera: Glossinidiae). *Insect. Biochem. Mol. Biol.* **33,** 1155–1164
2. Müller, S. (2004) Redox and antioxidant systems of the malaria parasite *Plasmodium falciparum*. *Mol. Microbiol.* **53,** 1291–1305
3. Akerman, S. E., and Müller, S. (2005) Peroxiredoxin-linked detoxification of hydroperoxides in *Toxoplasma gondii*. *J. Biol. Chem.* **280,** 564–570
4. Boveris, A., Sies, H., Martino, E. E., Docampo, R., Turrens, J. F., and Stoppani, A. O. (1980) Deficient metabolic utilization of hydrogen peroxide in *Trypanosoma cruzi*. *Biochem. J.* **188,** 643–648
5. He, S., Dayton, A., Kuppusamy, P., Werbovetz, K. A., and Drew, M. E. (2012) Induction of oxidative stress in *Trypanosoma brucei* by the antitrypanosomal dihydroquinoline OSU-40. *Antimicrob. Agents Chemother.* **56,** 2428–2434
6. Lüscher, A., de Koning, H. P., and Mäser , P. (2007) Chemotherapeutic strategies against *Trypanosoma brucei*: drug targets *vs.* drug targeting. *Curr. Pharm. Des.* **13,** 555–567
7. Müller, I. B., Das Gupta, R., Lüersen, K., Wrenger, C., and Walter, R. D. (2008) Assessing the polyamine metabolism of *Plasmodium falciparum* as chemotherapeutic target. *Mol. Biochem. Parasitol.* **160,** 1–7
8. Birkholtz, L. M., Williams, M., Niemand, J., Louw, A. I., Persson, L., and Heby, O. (2011) Polyamine homoeostasis as a drug target in pathogenic protozoa: peculiarities and possibilities. *Biochem. J.* **438,** 229–244
9. Krauth-Siegel, R. L., and Comini, M. A. (2008) Redox control in trypanosomatids, parasitic protozoa with trypanothione-based thiol metabolism. *Biochim. Biophys. Acta* **1780,** 1236–1248
10. Fairlamb, A. H., Blackburn, P., Ulrich, P., Chait, B. T., and Cerami, A. (1985) Trypanothione: a novel bis(glutathionyl)spermidine cofactor for glutathione reductase in trypanosomatids. *Science* **227,** 1485–1487
11. Arrick, B. A., Griffith, O. W., and Cerami, A. (1981) Inhibition of glutathione synthesis as a chemotherapeutic strategy for trypanosomiasis. *J. Exp. Med.* **153,** 720–725
12. Krieger, S., Schwarz, W., Ariyanayagam, M. R., Fairlamb, A. H., Krauth-Siegel, R. L., and Clayton, C. (2000) Trypanosomes lacking trypanothione reductase are avirulent and show increased sensitivity to oxidative stress. *Mol. Microbiol.* **35,** 542–552
13. Huynh, T. T., Huynh, V. T., Harmon, M. A., and Phillips, M. A. (2003) Gene knockdown of γ-glutamylcysteine synthetase by RNAi in the parasitic protozoa *Trypanosoma brucei* demonstrates that it is an essential enzyme. *J. Biol. Chem.* **278,** 39794–39800
14. Comini, M. A., Krauth-Siegel, R. L., and Flohé, L. (2007) Depletion of the thioredoxin homologue tryparedoxin impairs antioxidative defence in African trypanosomes. *Biochem. J.* **402,** 43–49
15. Barrett, M. P. (1997) The pentose phosphate pathway and parasitic protozoa. *Parasitol. Today* **13,** 11–16
16. Heise, N., and Opperdoes, F. R. (1999) Purification, localisation and characterisation of glucose-6-phosphate dehydrogenase of *Trypanosoma brucei*. *Mol. Biochem. Parasitol.* **99,** 21–32
17. Duffieux, F., Van Roy, J., Michels, P. A., and Opperdoes, F. R. (2000) Molecular characterization of the first two enzymes of the pentose-phosphate pathway of *Trypanosoma brucei*: glucose-6-phosphate dehydrogenase and 6-phosphogluconolactonase. *J. Biol. Chem.* **275,** 27559–27565
18. Igoillo-Esteve, M., Maugeri, D., Stern, A. L., Beluardi, P., and Cazzulo, J. J. (2007) The pentose phosphate pathway in *Trypanosoma cruzi*: a potential target for the chemotherapy of Chagas disease. *An. Acad. Bras. Cienc.* **79,** 649–663
19. Lee, S. H., Stephens, J. L., and Englund, P. T. (2007) A fatty-acid synthesis mechanism specialized for parasitism. *Nat. Rev. Microbiol.* **5,** 287–297
20. Barrett, M. P., and Gilbert, I. H. (2002) Perspectives for new drugs against trypanosomiasis and leishmaniasis. *Curr. Top. Med. Chem.* **2,** 471–482
21. Cordeiro, A. T., Thiemann, O. H., and Michels, P. A. (2009) Inhibition of *Trypanosoma brucei* glucose-6-phosphate dehydrogenase by human steroids and their effects on the viability of cultured parasites. *Bioorg. Med. Chem.* **17,** 2483–2489
22. Leroux, A. E., Maugeri, D. A., Opperdoes, F. R., Cazzulo, J. J., and Nowicki, C. (2011) Comparative studies on the biochemical properties of the malic enzymes from *Trypanosoma cruzi* and *Trypanosoma brucei*. *FEMS Microbiol. Lett.* **314,** 25–33
23. Brun, R., and Schönenberger (1979) Cultivation and *in vitro* cloning or procyclic culture forms of *Trypanosoma brucei* in a semi-defined medium. Short communication. *Acta Trop.* **36,** 289–292
24. Azema, L., Claustre, S., Alric, I., Blonski, C., Willson, M., Perié, J., Baltz, T., Tetaud, E., Bringaud, F., Cottem, D., Opperdoes, F. R., and Barrett, M. P. (2004) Interaction of substituted hexose analogues with the *Trypanosoma brucei* hexose transporter. *Biochem. Pharmacol.* **67,** 459–467
25. Ngô, H., Tschudi, C., Gull, K., and Ullu, E. (1998) Double-stranded RNA induces mRNA degradation in *Trypanosoma brucei*. *Proc. Natl. Acad. Sci. U.S.A.* **95,** 14687–14692
26. Bringaud, F., Robinson, D. R., Barradeau, S., Biteau, N., Baltz, D., and Baltz, T. (2000) Characterization and disruption of a new *Trypanosoma brucei* repetitive flagellum protein, using double-stranded RNA inhibition. *Mol. Biochem. Parasitol.* **111,** 283–297
27. Wirtz, E., Leal, S., Ochatt, C., and Cross, G. A. (1999) A tightly regulated inducible expression system for conditional gene knock-outs and dominant-negative genetics in *Trypanosoma brucei*. *Mol. Biochem. Parasitol.* **99,** 89–101
28. Coustou, V., Biran, M., Breton, M., Guegan, F., Rivière, L., Plazolles, N., Nolan, D., Barrett, M. P., Franconi, J. M., and Bringaud, F. (2008) Glucose-induced remodeling of intermediary and energy metabolism in procyclic *Trypanosoma brucei*. *J. Biol. Chem.* **283,** 16342–16354
29. Rivière, L., van Weelden, S. W., Glass, P., Vegh, P., Coustou, V., Biran, M., van Hellemond, J. J., Bringaud, F., Tielens, A. G., and Boshart, M. (2004) Acetyl:succinate CoA-transferase in procyclic *Trypanosoma brucei*. Gene identification and role in carbohydrate metabolism. *J. Biol. Chem.* **279,** 45337–45346
30. Klein, R. A., Linstead, D. J., and Wheeler, M. V. (1975) Carbon dioxide fixation in trypanosomatids. *Parasitology* **71,** 93–107
31. Harlow, E., and Lane, D. (eds) (1988) *Antibodies: A Laboratory Manual*, pp. 471–502, Cold Spring Harbor Laboratory Press, Cold Spring Harbor, NY
32. Sambrook, J., Fritsch, E. F., and Maniatis, T. (eds) (1989) *Molecular Cloning: A Laboratory Manual*, Chapters 18.47–18.74, Cold Spring Harbor Laboratory Press, Cold Spring Harbor, NY
33. Coustou, V., Biran, M., Besteiro, S., Rivière, L., Baltz, T., Franconi, J. M., and Bringaud, F. (2006) Fumarate is an essential intermediary metabolite produced by the procyclic *Trypanosoma brucei*. *J. Biol. Chem.* **281,** 26832–26846
34. Tetaud, E., Giroud, C., Prescott, A. R., Parkin, D. W., Baltz, D., Biteau, N., Baltz, T., and Fairlamb, A. H. (2001) Molecular characterisation of mitochondrial and cytosolic trypanothione-dependent tryparedoxin peroxidases in *Trypanosoma brucei*. *Mol. Biochem. Parasitol.* **116,** 171–183
35. Kohl, L., Sherwin, T., and Gull, K. (1999) Assembly of the paraflagellar rod and the flagellum attachment zone complex during the *Trypanosoma brucei* cell cycle. *J. Eukaryot. Microbiol.* **46,** 105–109
36. Ahmed, S. A., Gogal, R. M. Jr., and Walsh, J. E. (1994) A new rapid and simple non-radioactive assay to monitor and determine the proliferation of lymphocytes: an alternative to [^{3}H]thymidine incorporation assay. *J. Immunol. Methods* **170,** 211–224
37. Räz, B., Iten, M., Grether-Bühler, Y., Kaminsky, R., and Brun, R. (1997) The Alamar Blue assay to determine drug sensitivity of African trypanosomes (*T.b. rhodesiense* and *T.b. gambiense*) *in vitro*. *Acta Trop.* **68,** 139–147
38. Ebikeme, C., Hubert, J., Biran, M., Gouspillou, G., Morand, P., Plazolles, N., Guegan, F., Diolez, P., Franconi, J. M., Portais, J. C., and Bringaud, F. (2010) Ablation of succinate production from glucose metabolism in the procyclic trypanosomes induces metabolic switches to the glycerol 3-phosphate/dihydroxyacetone phosphate shuttle and to proline metabolism. *J. Biol. Chem.* **285,** 32312–32324
39. Bolten, C. J., Kiefer, P., Letisse, F., Portais, J. C., and Wittmann, C. (2007) Sampling for metabolome analysis of microorganisms. *Anal. Chem.* **79,** 3843–3849
40. Kiefer, P., Nicolas, C., Letisse, F., and Portais, J. C. (2007) Determination of carbon labeling distribution of intracellular metabolites from single fragment ions by ion chromatography tandem mass spectrometry. *Anal.*

Biochem. **360,** 182–188
41. Millard, P., Letisse, F., Sokol, S., and Portais, J. C. (2012) IsoCor: correcting MS data in isotope labeling experiments. *Bioinformatics* **28,** 1294–1296
42. Cannata, J. J., Frasch, A. C., Cataldi de Flombaum, M. A., Segura, E. L., and Cazzulo, J. J. (1979) Two forms of 'malic' enzyme with different regulatory properties in *Trypanosoma cruzi*. *Biochem. J.* **184,** 409–419
43. Orellano, E., and Cazzulo, J. J. (1981) Purification and regulatory properties of the NADP-linked malic enzyme for *Crithidia fasciculata*. *Mol. Biochem. Parasitol.* **3,** 1–11
44. Gupta, S., Cordeiro, A. T., and Michels, P. A. (2011) Glucose-6-phosphate dehydrogenase is the target for the trypanocidal action of human steroids. *Mol. Biochem. Parasitol.* **176,** 112–115
45. Ingram, A. K., Cross, G. A., and Horn, D. (2000) Genetic manipulation indicates that ARD1 is an essential N^{α}-acetyltransferase in *Trypanosoma brucei*. *Mol. Biochem. Parasitol.* **111,** 309–317
46. Mannaert, A., Downing, T., Imamura, H., and Dujardin, J. C. (2012) Adaptive mechanisms in pathogens: universal aneuploidy in *Leishmania*. *Trends Parasitol.* **28,** 370–376
47. Cronín, C. N., Nolan, D. P., and Voorheis, H. P. (1989) The enzymes of the classical pentose phosphate pathway display differential activities in procyclic and bloodstream forms of *Trypanosoma brucei*. *FEBS Lett.* **244,** 26–30
48. Creek, D. J., Chokkathukalam, A., Jankevics, A., Burgess, K. E., Breitling, R., and Barrett, M. P. (2012) Stable isotope-assisted metabolomics for network-wide metabolic pathway elucidation. *Anal. Chem.* **84,** 8442–8447
49. Pantopoulos, K., Mueller, S., Atzberger, A., Ansorge, W., Stremmel, W., and Hentze, M. W. (1997) Differences in the regulation of iron regulatory protein-1 (IRP-1) by extra- and intracellular oxidative stress. *J. Biol. Chem.* **272,** 9802–9808
50. Sureda, A., Hebling, U., Pons, A., and Mueller, S. (2005) Extracellular H_2O_2 and not superoxide determines the compartment-specific activation of transferrin receptor by iron regulatory protein 1. *Free Radic. Res.* **39,** 817–824
51. Mueller, S. (2000) Sensitive and nonenzymatic measurement of hydrogen peroxide in biological systems. *Free Radic. Biol. Med.* **29,** 410–415
52. Michels, P. A., Bringaud, F., Herman, M., and Hannaert, V. (2006) Metabolic functions of glycosomes in trypanosomatids. *Biochim. Biophys. Acta* **1763,** 1463–1477
53. Lamour, N., Rivière, L., Coustou, V., Coombs, G. H., Barrett, M. P., and Bringaud, F. (2005) Proline metabolism in procyclic *Trypanosoma brucei* is down-regulated in the presence of glucose. *J. Biol. Chem.* **280,** 11902–11910
54. van Weelden, S. W., Fast, B., Vogt, A., van der Meer, P., Saas, J., van Hellemond, J. J., Tielens, A. G., and Boshart, M. (2003) Procyclic *Trypanosoma brucei* do not use Krebs cycle activity for energy generation. *J. Biol. Chem.* **278,** 12854–12863
55. Bursell, E. (1981) The role of proline in energy metabolism. in *Energy Metabolism in Insects* (Downer, R. G. H., ed) pp. 135–154, Plenum Press, New York
56. Berriman, M., Ghedin, E., Hertz-Fowler, C., Blandin, G., Renauld, H., Bartholomeu, D. C., Lennard, N. J., Caler, E., Hamlin, N. E., Haas, B., Böhme, U., Hannick, L., Aslett, M. A., Shallom, J., Marcello, L., Hou, L., Wickstead, B., Alsmark, U. C., Arrowsmith, C., Atkin, R. J., Barron, A. J., Bringaud, F., Brooks, K., Carrington, M., Cherevach, I., Chillingworth, T. J., Churcher, C., Clark, L. N., Corton, C. H., Cronin, A., Davies, R. M., Doggett, J., Djikeng, A., Feldblyum, T., Field, M. C., Fraser, A., Goodhead, I., Hance, Z., Harper, D., Harris, B. R., Hauser, H., Hostetler, J., Ivens, A., Jagels, K., Johnson, D., Johnson, J., Jones, K., Kerhornou, A. X., Koo, H., Larke, N., Landfear, S., Larkin, C., Leech, V., Line, A., Lord, A., Macleod, A., Mooney, P. J., Moule, S., Martin, D. M., Morgan, G. W., Mungall, K., Norbertczak, H., Ormond, D., Pai, G., Peacock, C. S., Peterson, J., Quail, M. A., Rabbinowitsch, E., Rajandream, M. A., Reitter, C., Salzberg, S. L., Sanders, M., Schobel, S., Sharp, S., Simmonds, M., Simpson, A. J., Tallon, L., Turner, C. M., Tait, A., Tivey, A. R., Van Aken, S., Walker, D., Wanless, D., Wang, S., White, B., White, O., Whitehead, S., Woodward, J., Wortman, J., Adams, M. D., Embley, T. M., Gull, K., Ullu, E., Barry, J. D., Fairlamb, A. H., Opperdoes, F., Barrell, B. G., Donelson, J. E., Hall, N., Fraser, C. M., Melville, S. E., and El-Sayed, N. M. (2005) The genome of the African trypanosome *Trypanosoma brucei*. *Science* **309,** 416–422
57. Hannaert, V., Saavedra, E., Duffieux, F., Szikora, J. P., Rigden, D. J., Michels, P. A., and Opperdoes, F. R. (2003) Plant-like traits associated with metabolism of *Trypanosoma* parasites. *Proc. Natl. Acad. Sci. U.S.A.* **100,** 1067–1071
58. Coustou, V., Besteiro, S., Rivière, L., Biran, M., Biteau, N., Franconi, J. M., Boshart, M., Baltz, T., and Bringaud, F. (2005) A mitochondrial NADH-dependent fumarate reductase involved in the production of succinate excreted by procyclic *Trypanosoma brucei*. *J. Biol. Chem.* **280,** 16559–16570
59. Ghozlane, A., Bringaud, F., Soueidan, H., Dutour, I., Jourdan, F., and Thébault, P. (2012) Flux analysis of the *Trypanosoma brucei* glycolysis based on a multiobjective-criteria bioinformatic approach. *Adv. Bioinformatics* **2012,** 159423
60. Bringaud, F., Baltz, D., and Baltz, T. (1998) Functional and molecular characterization of a glycosomal PP_i-dependent enzyme in trypanosomatids: pyruvate, phosphate dikinase. *Proc. Natl. Acad. Sci. U.S.A.* **95,** 7963–7968
61. Suga, H., Matsuda, F., Hasunuma, T., Ishii, J., and Kondo, A. (2013) Implementation of a transhydrogenase-like shunt to counter redox imbalance during xylose fermentation in *Saccharomyces cerevisiae*. *Appl. Microbiol. Biotechnol.* **97,** 1669–1678
62. Naderer, T., Ellis, M. A., Sernee, M. F., De Souza, D. P., Curtis, J., Handman, E., and McConville, M. J. (2006) Virulence of *Leishmania major* in macrophages and mice requires the gluconeogenic enzyme fructose-1,6-bisphosphatase. *Proc. Natl. Acad. Sci. U.S.A.* **103,** 5502–5507
63. Garami, A., and Ilg, T. (2001) Disruption of mannose activation in *Leishmania mexicana*: GDP-mannose pyrophosphorylase is required for virulence, but not for viability. *EMBO J.* **20,** 3657–3666
64. McConville, M. J., and Naderer, T. (2011) Metabolic pathways required for the intracellular survival of *Leishmania*. *Annu. Rev. Microbiol.* **65,** 543–561
65. Jiang, P., Du, W., Mancuso, A., Wellen, K. E., and Yang, X. (2013) Reciprocal regulation of p53 and malic enzymes modulates metabolism and senescence. *Nature* **493,** 689–693
66. Bringaud, F., Barrett, M. P., and Zilberstein, D. (2012) Multiple roles of proline transport and metabolism in trypanosomatids. *Front. Biosci.* **17,** 349–374

Cytosolic NADPH Homeostasis in Glucose-starved Procyclic *Trypanosoma brucei* Relies on Malic Enzyme and the Pentose Phosphate Pathway Fed by Gluconeogenic Flux

Stefan Allmann, Pauline Morand, Charles Ebikeme, Lara Gales, Marc Biran, Jane Hubert, Ana Brennand, Muriel Mazet, Jean-Michel Franconi, Paul A. M. Michels, Jean-Charles Portais, Michael Boshart and Frédéric Bringaud

J. Biol. Chem. 2013, 288:18494-18505.
doi: 10.1074/jbc.M113.462978 originally published online May 10, 2013
